PHYSICAL REVIEW B **77**, 241404(R) (2008)

Pit formation during graphene synthesis on SiC(0001): *In situ* electron microscopy

J. B. Hannon* and R. M. Tromp
IBM Research Division, T. J. Watson Research Center, Yorktown Heights, New York 10598, USA
(Received 28 April 2008; revised manuscript received 3 June 2008; published 26 June 2008)

We have studied the formation of graphene on the Si face of SiC(0001)-6H and -4H using *in situ* electron microscopy. By imaging the nucleation and growth of the $6\sqrt{3}$ "buffer layer" during annealing in vacuum we identify key factors responsible for the appearance of deep pits during graphene formation. Pits form because domains of the buffer layer pin decomposing surface steps. Graphene is observed to nucleate in the pits, where the step density is high.

DOI: 10.1103/PhysRevB.77.241404 PACS number(s): 61.46.−w

The unique electronic properties of graphene[1] have spurred interest in potential applications in nanoelectronics.[2] For most of the envisioned device structures, graphene films must be grown or placed on semi-insulating substrates. One approach is to anneal SiC(0001) surfaces at high temperature.[3] When heated above 1050 °C, Si preferentially desorbs, leaving behind a C-rich overlayer from which graphene can be formed. For many applications, flat, uniform, graphene films of only a few layers are desired. However, on the Si face of SiC(0001) several groups have observed the formation of pits during graphene synthesis.[4,5] These pits hinder the formation of flat graphene films at temperatures below 1200 °C. In this Rapid Communication we describe experiments designed to probe how and why pits form, and to determine how pit formation depends on processing conditions. Using low-energy electron microscopy (LEEM), we have imaged the Si face of both *N*-doped SiC(0001)-6H and intrinsic SiC(0001)-4H during high-temperature annealing in ultrahigh vacuum (UHV). By observing how the C-rich $6\sqrt{3}$ buffer layer forms we identify two key factors responsible for pit formation: (1) the stability of the buffer layer with respect to the surrounding SiC ($\sqrt{3}$ phase), and (2) the fact that the SiC surface decomposes exclusively at steps, causing the steps to retract *around* $6\sqrt{3}$ domains. The pinning of SiC steps at buffer layer domains is the primary mechanism by which pits form at temperatures below 1200 °C. At higher temperature, nucleation of holes in the $\sqrt{3}$ phase is also observed. These factors suggest that pit formation during low-temperature graphene growth in UHV is an intrinsic feature of Si-terminated SiC(0001).

The structure of SiC(0001) corresponds to a stacking of hexagonal SiC bilayers with an interlayer spacing of 0.25 nm. Our experiments were carried out on the Si face, in which the Si atoms in each bilayer are uppermost. Experiments on doped-6H and intrinsic-4H samples showed similar behavior. Here we focus mainly on results from the -6H surface. We cleaned the surfaces in ultrahigh vacuum by exposing to disilane in the range 700 °C–800 °C. Temperatures were measured by calibrating the heating power using an optical pyrometer. The temperatures at which various surface phases appear agree well with previous investigations.[6,7] After cleaning, single-height steps were observed in LEEM. However, prolonged annealing at 1025 °C leads to the formation of steps with a step height equal to three SiC bilayers on -6H samples.[8] An *ex situ* atomic-force microscopy (AFM) image from a starting -6H surface is shown in Fig. 1(a). Typically, our AFM measurements are made within 30 min of removing a sample from UHV. The steps are smooth, with a step height of 0.8 nm, corresponding to three SiC bilayers (0.754 nm). The evolution toward triple-height steps shows that -6H surfaces with different bilayer terminations have different surface energies, and that one particular surface termination (e.g., the plane at the stacking fault) is favored.

After exposure to disilane at 900 °C, the Si-rich 3×3 phase was formed. A 1×1 diffraction pattern was observed when the surface was heated above 1000 °C, followed by a $\sqrt{3}\times\sqrt{3}$ structure at about 1050 °C. Further annealing leads to the appearance of the $6\sqrt{3}\times6\sqrt{3}-R30°$ buffer layer phase at 1060 °C.

The buffer layer phase is bright in the 18 eV LEEM image and nucleates primarily at the lower sides of atomic steps [Fig. 1(b)]. The buffer layer can be identified using selected area diffraction and dark-field imaging. While the diffraction pattern of the buffer layer is consistent with double diffraction from a graphene layer on 1×1 SiC(0001),[3] scanning tunneling microscope (STM) measurements suggest that the room-temperature structure is more complex.[7,9,10]

AFM imaging gives some insight into how the buffer layer forms. An image from the surface before nucleation of the buffer layer is shown in Fig. 1(a). An AFM image recorded after the buffer layer nucleates is shown in Fig. 1(c). It is clear that the step structure has been perturbed by nucleation of the buffer layer. The steps are no longer atomically smooth, and part of the upper side of the step has been eaten away. Notably, the terraces are not etched, only the step edges. The etched areas are uniformly 0.8 nm deep. That is, SiC at the step decomposes in units of *three* bilayers. The lower sides of the steps have an extended "ribbon" of material that grows out onto the lower terrace. In addition, islands (indicated by arrows) are seen near the centers of the terraces.

Comparison of the images in Fig. 1 shows that the buffer layer phase imaged in LEEM corresponds to the islands and ribbons imaged with AFM. Analysis of AFM images indicates that the buffer layer is about 0.2 nm thick. The homogeneous nucleation of buffer layer islands on the terraces shows clearly that carbon can diffuse freely, and that the supersaturation of C at 1060 °C is relatively large.

The only morphological change at the surface is the etching of the steps—no terrace pits are seen in AFM—

 ©2008 The American Physical Society

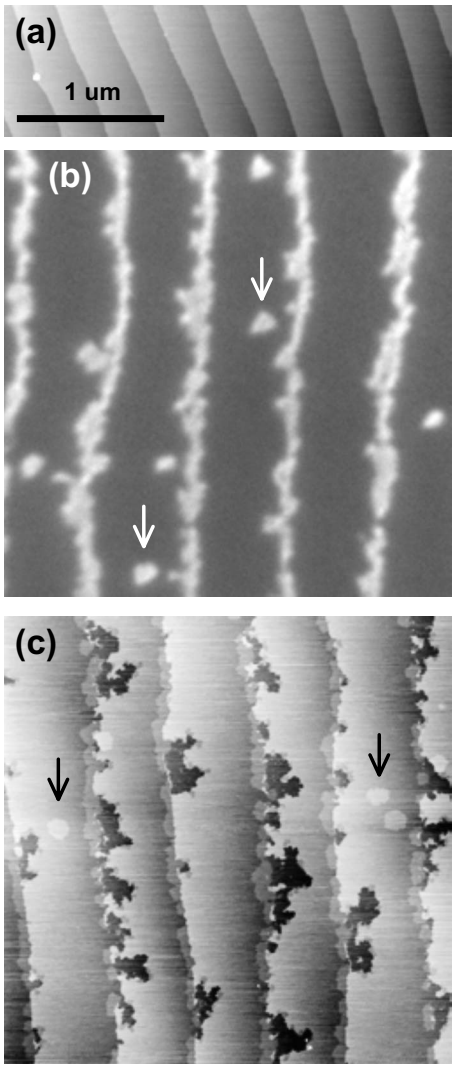

FIG. 1. Nucleation of the $6\sqrt{3}$ buffer layer on SiC(0001)-6H-$\sqrt{3}\times\sqrt{3}$ at 1060 °C. (a) AFM image of the surface before nucleation with 0.8 nm high steps. (b) 18 eV bright field LEEM image recorded after nucleation of the buffer layer at 1060 °C. The buffer layer is bright and the $\sqrt{3}$ phase is dark. (c) AFM image from the same surface showing islands, ribbons at the lower sides of the steps, and etched step edges. The arrows indicate buffer layer domains that have nucleated on the terrace.

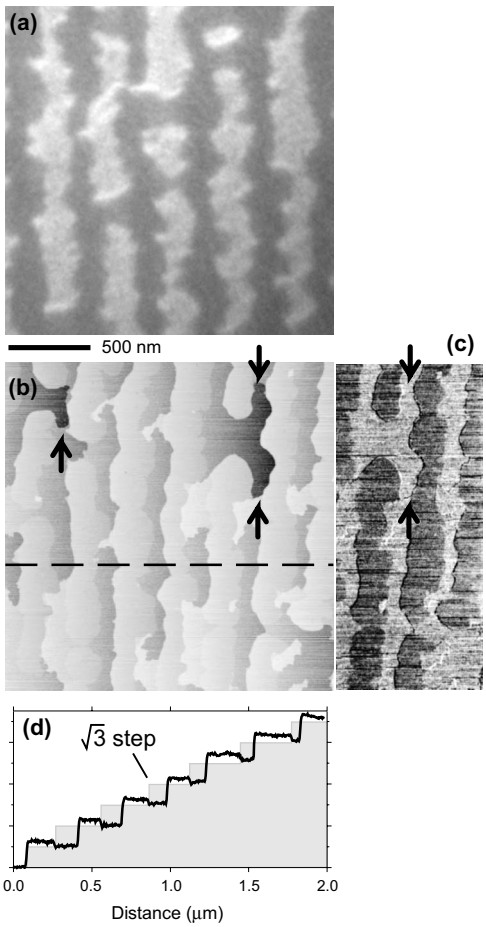

FIG. 2. (a) 5.3 eV bright field LEEM image at 1140 °C of large buffer layer domains (bright). (b) AFM image from the same surface illustrating the flow of $\sqrt{3}$ steps around the buffer layer (arrows). (c) AFM phase image from the right of (b) showing contrast between buffer layer (dark) and $\sqrt{3}$ (bright). (d) Line scan from the dotted line indicated in (b). Tall steps (left) are 1.0 nm and short steps (right) are 0.2 nm. The schematic starting profile is shown in gray.

suggesting that the carbon in the buffer layer comes from the decomposition of the $\sqrt{3}$ terraces.[11] The carbon content of three SiC bilayers is 37 atoms/nm^2. In Fig. 1(c), about 10% of the surface has decomposed, while 11% is covered by the buffer layer phase, suggesting that the carbon content of the buffer layer is similar, and comparable to that of graphene (38 atoms/nm^2).[12]

Analysis of the later stages of growth gives some insight into the stability of the buffer layer. The buffer layer first appears at the step edges at about 1060 °C. When the surface is annealed at higher temperature, the area of the surface covered by the buffer layer increases. Images recorded after annealing to 1140 °C are shown in Fig. 2. The LEEM image shows that the domains of the buffer layer are wider, covering about half of the terrace. AFM topography and phase images are shown in Figs. 2(b) and 2(c). The phase image [Fig. 2(c)] shows strong contrast between the buffer layer (imaged dark) and the $\sqrt{3}$ phase (bright). The topography image makes clear that the domains of the buffer layer are no longer located at the lower side of the $\sqrt{3}$ steps. Rather, the buffer layer is now located at the *upper* sides of the steps—that is, nearly all of the $\sqrt{3}$ steps have been replaced by steps with the buffer layer phase on the upper side.

The images in Fig. 1 show that the buffer layer grows at the expense of $\sqrt{3}$ steps. The images from the later stages of growth show that the $\sqrt{3}$ steps continue to decompose, retracting away from the buffer layer domains. Areas marked with arrows in Figs. 2(b) and 2(c) show places where a $\sqrt{3}$ step has retracted around an existing buffer layer domain and has crossed onto the neighboring "uphill" terrace. When the retracting step reaches the buffer layer, the decomposition stops and the buffer layer ceases to grow. Continued growth of the buffer layer requires a new source of carbon, e.g., from the nucleation of holes in the $\sqrt{3}$ terraces.

The carbon density in the buffer layer is nearly the same

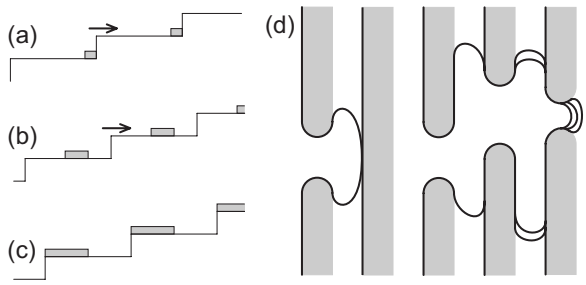

FIG. 3. Model of $6\sqrt{3}$ growth on SiC(0001)-$\sqrt{3}$. (a) The buffer layer (gray) nucleates at the lower sides of $\sqrt{3}$ steps. (b) $\sqrt{3}$ steps retract uphill as the buffer layer grows. (c) Eventually a state is reached in which all $\sqrt{3}$ steps have been consumed, and with the buffer layer covering roughly half of the surface. (d) Canyons or pits form when the domains of the buffer layer on each terrace are not continuous and $\sqrt{3}$ steps (thick black lines) advance to the next terrace.

as that of three SiC bilayers. Therefore, when all of the $\sqrt{3}$ steps are consumed, the buffer layer should cover about half the surface.[12] This is approximately the case in the line scan indicated in Fig. 2(b) and shown in Fig. 2(d). The average step height on the left side of the domains is 1.00 ± 0.03 nm and that on the right is 0.18 ± 0.04 nm, consistent with the three SiC bilayers (0.76 nm) and a buffer layer thickness of 0.2 nm. Using this information, we can infer what the original step structure of the SiC surface was before the buffer layer nucleated. This schematic reconstruction is shown in gray in Fig. 2(d). Gray areas *above* the black line represent SiC that has decomposed while white regions *below* the black line indicate where the buffer layer has grown.

A schematic of how the growth proceeds is shown in Fig. 3. At 1050 °C the buffer layer nucleates, primarily at steps [Fig. 3(a)]. With further annealing, the buffer layer grows, and the $\sqrt{3}$ steps retract uphill [Fig. 3(b)]. Eventually a frustrated state similar to that indicated in Fig. 2 is reached in which all $\sqrt{3}$ steps have been consumed, and the buffer layer covers roughly half the surface. In the absence of a new carbon source, growth of the buffer layer stops.

If the buffer layer is not continuous on each terrace, the simple morphology shown in Fig. 3(c) does not result. If there are gaps in the buffer layer, as seen in Fig. 2, then the $\sqrt{3}$ steps continue to retract onto the next uphill terrace. This results in a double-height step at the next buffer layer domain, as shown in the left side of Fig. 3(d). If there are even more gaps, the $\sqrt{3}$ steps can retract even further, leading to the formation of deep canyons with large macrosteps at the uphill side, as shown at the right of Fig. 3(d). The migration of steps through gaps in the buffer layer is the primary pit-nucleation mechanism below 1150 °C.

We have observed canyon formation in LEEM during slow heating, when the density of buffer layer domains is low. The LEEM image in Fig. 4(a) was recorded at 1160 °C, after the buffer layer growth rate had slowed, presumably due to the absence of $\sqrt{3}$ steps. Note that the remaining $\sqrt{3}$ areas (dark) span several terraces, and that steps curve around them, suggesting that the dark areas are the pits depicted in Fig. 3(d). When this surface is heated above about 1150 °C, new domains of the buffer layer nucleate in the

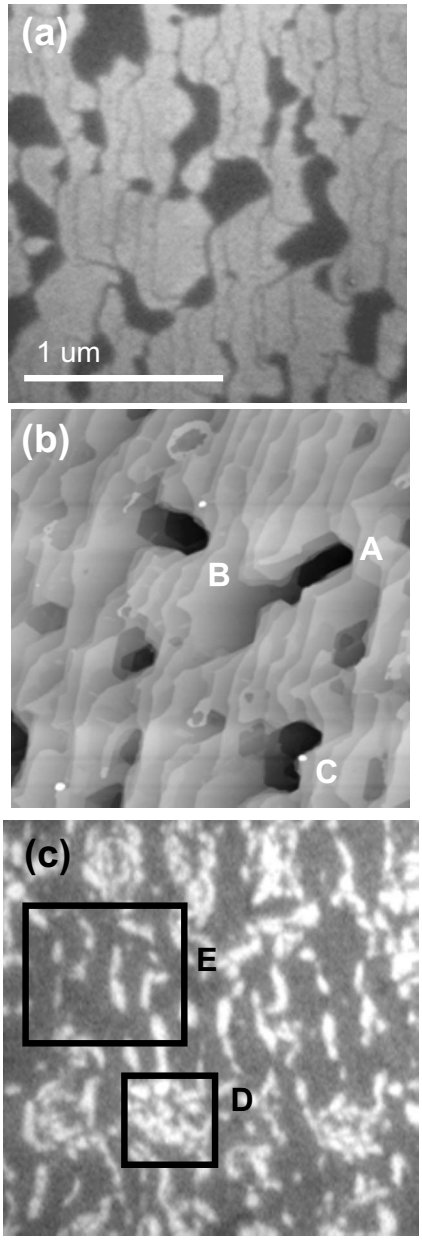

FIG. 4. (a) 3 eV bright field LEEM image recorded at 1150 °C before the completion of the buffer layer. (b) AFM image after heating to 1250 °C. The canyons marked *A*, *B*, and *C* are 6 nm deep (or 8 SiC bilayers). Vacancy islands have nucleated in the bottoms of the canyons, increasing their depth. (d) 19 eV bright field LEEM image recorded after graphene formation at 1160 °C. Graphene is bright in the image and nucleates preferentially in areas of high step density, e.g., in the canyons (*D*).

remaining $\sqrt{3}$ areas. AFM imaging shows that new pits (one monolayer deep) have nucleated preferentially *inside* preexisting pits. Examples are indicated in Fig. 4(b).

Heating above 1160 °C results in the formation of a second carbon layer. *In situ* photoelectron spectroscopy shows that this new phase has the band structure of graphene. Furthermore, using the method described by Hibino *et al.*,[13] we confirmed that the new phase corresponds to one graphene layer (on the buffer layer) by measuring the energy dependence of the reflectivity. In LEEM, we observe graphene

nucleation primarily at steps and, notably, in the canyons where the step density is highest. An AFM image after annealing above 1200 °C is shown in Fig. 4(b). Features marked *A*, *B*, and *C* are canyons with a step height of at least 6 nm (8 SiC bilayers) at the uphill side. Clearly the canyons survive at temperatures where graphene layers start to form. The LEEM image in Fig. 4(c) was obtained from a different sample annealed above 1200 °C. LEEM imaging shows that the graphene nucleates predominantly in the canyons (e.g., the boxed area labeled *D* in Fig. 4(c) is a region of high step density and is probably a pit) but also at steps in the flatter areas (*E*). The domain size is small, especially in pits, where the step density is highest. Clearly the pitted surface morphology influences how graphene nucleates.

In summary, we have imaged the evolution of SiC(0001) (Si-termination) surface morphology during annealing above 1200 °C. Although the starting surface consists of a well-ordered array of straight steps, the state of the surface when graphene forms is rough. The steps are no longer straight and deep pits are observed. Pit formation is traced to the stability of the buffer layer at 1060 °C and the existence of gaps in the buffer layer coverage on each terrace. Below 1200 °C, the buffer layer is essentially static. Our results suggest that rapid nucleation of the buffer layer, to minimize the formation of gaps, would inhibit pit formation. During slow annealing to high temperature, the nucleation density is low. The domains grow fairly large, but are widely spaced along the step, with the gaps between domains leading to pit formation (as shown in Fig. 3). Rapid, high-temperature annealing presumably results in a higher nucleation density, with many small, closely-spaced domains at the steps. Gaps between domains would be smaller, and the tendency to form pits would be lower. However, the growth of smooth, flat graphene films may require annealing at temperatures well above 1200 °C, where multiple layers of graphene may form.

*jbhannon@us.ibm.com

[1] A. Geim and K. Novoselov, Nat. Mater. **6**, 183 (2007).

[2] C. Berger *et al.*, J. Phys. Chem. B **108**, 19912 (2004).

[3] A. van Bommel, J. Crombeen, and A. van Tooren, Surf. Sci. **48**, 463 (1975).

[4] V. Derycke, R. Martel, M. Radosavljevic, F. Ross, and P. Avouris, Nano Lett. **2**, 1043 (2002).

[5] G. Gu, S. Nie, R. M. Feenstra, R. P. Devaty, W. J. Choyke, W. K. Chan, and M. G. Kane, Appl. Phys. Lett. **90**, 253507 (2007).

[6] I. Forbeaux, J. M. Themlin, and J. M. Debever, Phys. Rev. B **58**, 16396 (1998).

[7] W. Chen, H. Xu, L. Liu, X. Gao, D. Qi, G. Pend, S. C. Tan, Y. Feng, K. P. Loh, and A. T. Wee, Surf. Sci. **596**, 176 (2005).

[8] Dark-field LEEM imaging shows that the diffraction pattern on neighboring terraces is rotated by 180° for both −6*H* and −4*H* samples. This rotation is expected if the step height is half the height of the unit cell.

[9] F. Owman and P. Mårtensson, Surf. Sci. **369**, 126 (1996).

[10] W. J. Ong and E. S. Tok, Phys. Rev. B **73**, 045330 (2006).

[11] Diffraction measurements (Ref. 14) and first-principles electronic structure calculations (Ref. 15) suggest that the $\sqrt{3}\times\sqrt{3}$ phase has the same carbon density as the 1×1 phase.

[12] During the initial nucleation of the buffer layer (Fig. 1), it appears that carbon is locally conserved. That is, the buffer layer forms from carbon released from nearby $\sqrt{3}$ steps. At the later stages of growth, this is no longer the case, implying long-range diffusion of carbon on the surface from $\sqrt{3}$ steps to existing buffer layer domains.

[13] H. Hibino, H. Kageshima, F. Maeda, M. Nagase, Y. Kobayashi, and H. Yamaguchi, Phys. Rev. B **77**, 075413 (2008).

[14] Y. Han, T. Aoyama, A. Ichimiya, Y. Hisada, and S. Mukainakano, J. Vac. Sci. Technol. B **19**, 1972 (2001).

[15] J. E. Northrup and J. Neugebauer, Phys. Rev. B **52**, R17001 (1995).